EBioMedicine 20 (2017) 50–60

Contents lists available at ScienceDirect

EBioMedicine

journal homepage: www.ebiomedicine.com

Research Paper

BCKDK of BCAA Catabolism Cross-talking With the MAPK Pathway Promotes Tumorigenesis of Colorectal Cancer

Peipei Xue [a,1], Fanfan Zeng [a,1], Qiuhong Duan [a,1], Juanjuan Xiao [a], Lin Liu [a], Ping Yuan [a], Linni Fan [c], Huimin Sun [b], Olesya S. Malyarenko [a,e], Hui Lu [a], Ruijuan Xiu [a], Shaoqing Liu [d], Chen Shao [b], Jianmin Zhang [a], Wei Yan [c,*], Zhe Wang [c,*], Jianyong Zheng [d,*], Feng Zhu [a,*]

[a] Department of Biochemistry and Molecular Biology, School of Basic Medicine, Huazhong University of Science and Technology, Wuhan, Hubei 430030, PR China
[b] Department of Urology, Xijing Hospital, The Fourth Military Medical University, Xi'an, Shaanxi 710032, PR China
[c] Department of Pathology, Xijing Hospital, The Fourth Military Medical University, Xi'an, Shaanxi 710032, PR China
[d] Department of State Key Laboratory of Cancer Biology, Xijing Hospital, The Fourth Military Medical University, Xi'an, Shaanxi 710032, PR China
[e] G.B. Elyakov Pacific Institute of Bioorganic Chemistry, Far Eastern Branch of Russian Academy of Sciences, Laboratory of Enzyme Chemistry, Vladivostok, Russia

ARTICLE INFO

Article history:
Received 8 January 2017
Received in revised form 1 May 2017
Accepted 1 May 2017
Available online 4 May 2017

Keywords:
Branched-chain amino acids catabolism
Colorectal cancer
BCKDK
Tumorigenesis
MEK
Phenyl butyrate

ABSTRACT

Branched-chain amino acids catabolism plays an important role in human cancers. Colorectal cancer is the third most commonly diagnosed cancer in males and the second in females, and the new global incidence is over 1.2 million cases. The branched-chain α-keto acid dehydrogenase kinase (BCKDK) is a rate-limiting enzyme in branched-chain amino acids catabolism, which plays an important role in many serious human diseases. Here we investigated that abnormal branched-chain amino acids catabolism in colorectal cancer is a result of the disease process, with no role in disease initiation; BCKDK is widely expressed in colorectal cancer patients, and those patients that express higher levels of BCKDK have shorter survival times than those with lower levels; BCKDK promotes cell transformation or colorectal cancer *ex vivo* or *in vivo*. Mechanistically, BCKDK promotes colorectal cancer by enhancing the MAPK signaling pathway through direct MEK phosphorylation, rather than by branched-chain amino acids catabolism. And the process above could be inhibited by a BCKDK inhibitor, phenyl butyrate.

1. Introduction

Tumor metabolism is closely related to tumorigenesis and tumor progression (Burrage et al., 2014; Gill et al., 2016; Nelson et al., 2013; Pike et al., 2011; Sonnet et al., 2016; Watanabe et al., 1984). Gill et al. (2016) presented that the increased rate of glycolysis can support cancer cells rapid proliferation through fulfilling cells biosynthetic demands. Pike et al. (2011) showed fatty acid oxidation promotes cancer cells growth and survival through providing bioenergetic fuel for cells. Nelson et al. (2013) demonstrated a primary metabolite of cholesterol, 27-hydroxycholesterol (27HC), promotes tumor cells growth and metastasis through signal transduction. The above studies show that the metabolism effects tumor growth in 3 ways: providing biosynthetic materials, providing energy, or through signal transduction. Branched-chain amino acids (BCAA) catabolism is abnormal in many human diseases (Burrage et al., 2014; Sonnet et al., 2016; Watanabe et al., 1984). Branched-chain amino transferase (BCAT) is the first enzyme in BCAA catabolism which has a higher activity in tumors and has been shown to be a useful marker for grading and genetic characterization in glioma, colorectal cancer (CRC) and medulloblastoma (Conway et al., 2016; de Bont et al., 2008; Mitchell et al., 2014). However, healthy human prostate tissue was found to have elevated BCAT levels relative to malignant tissue (Billingsley et al., 2014). Therefore, the role of BCAA catabolism in tumors need to be further understood.

BCKDK is a key negative regulation enzyme in BCAA catabolism that inhibits the dehydrogenase activity of the branched-chain α-keto acid dehydrogenase (BCKDH) complex by dephosphorylating the E1 component of the complex (Chuang et al., 2002). BCKDK plays an important role in many serious human diseases, including Huntington's disease (Mochel et al., 2007), Maple syrup urine disease (Beaudet, 2012;

Abbreviations: BCAA, branched-chain amino acids; BCKDK, branched-chain α-keto acid dehydrogenase kinase; CRC, colorectal cancer; BCAT, branched- chain amino transferase; 27HC, 27-hydroxycholesterol; BCKA, branched- chain α-keto acid; BCKDHA, branched-chain α-keto acid dehydrogenase E1; ERK, extracellular signal-regulated kinase; MAPK, mitogen-activated protein kinase; PB, phenylbutyrate.

* Corresponding authors.
E-mail addresses: yan070@sina.com (W. Yan), zhwang@fmmu.edu.cn (Z. Wang), zhengjy@fmmu.edu.cn (J. Zheng), fengzhu@hust.edu.cn (F. Zhu).

[1] Peipei Xue, Fanfan Zeng and Qiuhong Duan contributed equally to this article and should be considered as co-first authors.

http://dx.doi.org/10.1016/j.ebiom.2017.05.001

Sonnet et al., 2016), human autism with Epilepsy (Novarino et al., 2012), and Obesity (Burrage et al., 2014). However, the relationship between BCKDK and cancer is unknown.

CRC is the third most commonly diagnosed cancer in males and the second in females, and the new global incidence is over 1.2 million cases (Torre et al., 2015). Therefore, the mechanism of CRC tumorigenesis need to be further elucidated. Watanabe et al. (1984) reported that BCAA levels in the tumor tissue of colon cancers were generally higher than those in the respective nontumorous tissue. On the other hand, Wubetu et al. (2014) showed BCAA suppressed insulin-initiated proliferation of human Colon tumor cells through induction of autophagy. Yoshikawa et al. (2006) demonstrated BCAT1 over-expression is a sensitive marker of metastasis in CRC. Therefore, the role of BCAA catabolism in CRC is controversial. BCAA is a biosynthetic material, however, whether BCAA is a potential carcinogen is unclear.

In this study, we identify BCKDK as an upstream kinase of MEK. We show that the BCKDK positively regulates MEK/ERK signaling by directly phosphorylating MEK at Ser221. BCKDK has a higher expression in the colorectal tissues of CRC patients *versus* normal tissues. The higher that BCKDK is expressed, the shorter survival time is in CRC patients. Over-expression of BCKDK increases the clone formation of JB6 Cl41 and WiDr cells *ex vivo.* Knockdown of BCKDK inhibits colorectal tumor progression *ex vivo* and *in vivo*. The above suggests BCAA catabolism can crosstalk with MAPK signaling pathway, whereby BCKDK plays a crucial role in human CRC tumorigenesis through phosphorylating MEK at ser221.

2. Materials and Methods

2.1. Plasmids, shRNA, Antibodies, and Other Reagents

The plasmids of pBABEpuro-HA-MEK1 (catalog: 53195) and pDONR223-BCKDK (catalog: 23,794) were purchased from Addgene (Cambridge, MA, USA). The plasmid of pCMV-C-Flag (catalog: D2632) was purchased from Beyotime Biotechnology (Shanghai, China). The plasmid of pCMV-Myc (catalog: 631604) was purchased from Clontech Laboratories, Inc. (Mountain View, CA, USA). The plasmid of pET23a-His (catalog: 69745-3) was purchased from Novagen (Darmstadt, Hessen, Germany). The plasmids of pCMV-BCKDK-Flag, pCMV-Myc-MEK1, pET23a-MEK1 (residues 62-393)-His, and pLKO.1-shBCKDK were constructed by our laboratories. The sense template sequence for BCKDK amplification was 5′-CGGAATTCCGATGATCCTGG.

CGTCGGTGCTGAGG-3′ (*Eco*RI end underlined) and the antisense template sequence was 5′-CCGCTCGAGGATCCGGAAGCTTTCCTCCCGGCC-3′ (*Xho*I end underlined). The amplified BCKDK and pCMV-c-Flag vector were digested with *Eco*RI and *Xho*I, ligation, and colony screening for pCMV-BCKDK-Flag. The sense template sequence for MEK1 amplification was 5′-CCGCTCGAGCGCCCAAGAAG AAGCCGACG-3′ (*Xho*I end underlined) and the antisense template sequence was 5′-ATAAGAATGCGGCCGCTTAAGCCAAATGGTGGAGCCAG-3′ (*Not*I end underlined). The amplified MEK1 was cloned into pCMV-Myc vector at *Xho*I and *Not*I sites. The sense template sequence for MEK1 (residues 62-393) amplification was 5′-CGGGATCCCGGAAGCGCCT TGAGGCCTTTCTGAC-3′ (*Bam*HI end underlined) and the antisense template sequence was 5′-CCGCTCGAGAGCCAAATGGTGGAGCCAGATC-3′ (*Xho*I end underlined). The amplified MEK1 (residues 62-393) was cloned into pet23a-his vector at *Bam*HI and *Xho*I sites. 5 sequences were designed to knock down BCKDK, and the sequences are: 1. 5′-CCGGCGTCCGCTACTTCTTGGACAACTCGAGTTGTCCAAGAAGTAGCGGAC-GTTTTTG-3′; 2. 5′-CCGGCCAGCACCAGTTCCGTCATTCCTCGAGGAATGA CGGAACTGGTGCTGGTTTTTG-3′; 3. 5′-CCGGGATCTGATCATCAGGATCTCA CTCGAGTGAGATCCTGATGATCAGATCTTTTTG-3′; 4. 5′-CCGGTCAGGACCC ATGCACGGCTTTCTCGAGAAAGCCGTGCATGGGTCCTGATTTTTG-3′; 5. 5′-C CGGACGCTGACTTCGAGGCTTGGACTCGAGTCCAAGCCTCGAAGTCAGCGT-TTTTTG-3′. A mock shRNA with a sequence lacking significant homology to the human genome database was used as the mock shRNA. The sequence was: 5′-CCGG

CCTAAGGTTAAGTCGCCCTCGCTCGAGCGAGGGCGACTTAACCTTAGG-TTTTTG-3′. The sense and anti-sense oligonucleotides were synthesized, annealed and cloned into the pLKO.1-TRC cloning vector at the *Eco*RI and *Age*I sites as described by the manufacturer (Moffat et al., 2006).

Anti-mouse BCKDK antibody (catalog: sc-374425) and anti-β-actin antibody (catalog: sc-130656) were purchased from Santa Cruz Technology, Inc. (Santa Cruz, CA, USA). Anti-p-MEK1/2 (ser221) (catalog: 2338), phospho-p44/42MAPK (Erk1/2) (T202/Y204) (D13.14.4E) (catalog: 4370), t-MEK (catalog: 8727), and t-ERK (catalog: 4695) antibodies were purchased from Cell Signaling Technology (Danvers, MA, USA). Anti-Flag antibody (catalog: F1804, catalog: F7425) was purchased from Sigma-Aldrich (St. Louis, MO, USA). HRP-conjugated anti-mouse antibody (catalog: E030110) and HRP-conjugated anti-rabbit (catalog: E030120) antibody were purchased from EarthOx Life Sciences (San Francisco, CA, USA). Simple-Fect (catalog: Profect-01) was purchased from Signaling Dawn Biotech (Wuhan, Hubei, China) for transfection. G418 (catalog: A1720) and puromycin were purchased from Sigma-Aldrich (St. Louis, MO, USA) and used for setting up stable cell lines.

2.2. Cell Culture

The human colon cancer cell lines (DLD1, HCT8, SW480, WiDr, HCT116, and HCT15) and the normal cell lines (HIEC-6, JB6 C141, and HEK293T) were purchased from American Type Culture Collection (ATCC; Manassas, VA, USA).

2.3. Western Blot

Cells ($0.8–2 \times 10^6$) were cultured in 10 cm diameter dishes to 70–80% confluence, and then starved no serum for either 12 h (JB6 C141 cell lines) or 24 h (colon cancer cell lines). The cells were then treated with 20 ng/mL epidermal growth factor (EGF) (R&D catalog: 236-EG-200) for 15 min. EGF is a well-known tumor promotion agent used to study malignant cell transformation in animal and cell models of cancer (Hunter and Karin, 1992; Sachsenmaier et al., 1994; Sassone-Corsi et al., 1999; Scafidi et al., 2014). After this, cells were washed once in PBS before being lysed in RIPA buffer (1 × PBS, 1% NP-40, 0.1% SDS, 0.5% sodium deoxycholate, 1 mmol/L Na3VO4, 1 mmol/L aprotinin and 1 mmol/L phenylmethylsulfonyl fluoride). In addition, HCT116 cells were treated with 0–3200 μM BCKDK inhibitor for 48 h, with the later 24 h together with no serum. Then, samples were sonicated in 15 second intervals three times, and insoluble debris was removed by centrifugation at 13000 rpm for 15 min. Protein content was determined by Bradford method (Bradford, 1976). 30–120 μg of protein was separated by 10% SDS-PAGE and visualized by chemiluminescence (BIO-RAD, USA) in triplicate.

2.4. Growth Curve Analysis and MTS Assays

2×10^5 cells were plated in each dish and counted at different times in triplicate, using a hemacytometer to generate a growth curve. For inhibition assays, 1×10^3 HCT116 cells were seeded in 96-well plates for 24 h, and then cells were fed with fresh medium containing different concentrations of BCKDK inhibitor, phenyl butyrate (PB), for 48 h. The cytotoxicity of inhibitors was measured with MTS assay kit (Promega catalog: G3580) according to the manufacturer's instructions in triplicate, with the results expressed as the percentage of inhibition.

2.5. Bacterial Expression and Purification of the MEK1-His

The pET23a-mek1 (residues 62-393)-his plasmid was expressed in *E. coli* BL21 bacteria (Novagen; Darmstadt, Hessen, Germany). Bacteria were grown at 37 °C overnight. Then, bacteria were harvested by

centrifugation at 3000 rpm. The pellets were washed with PBS 5 times, and were disrupted by sonication. The lysate was again centrifuged, and the new pellets were washed by PBS for another 5 times. The clean pellets were then dissolved with a minimum volume of 8 M Urea buffer (8 M Urea, 50 mM Tris, 0.5 M NaCl, 0.5%Triton-100, pH 8.0). The protein in supernatant was saved, and diluted to 1 M Urea buffer for use.

2.6. Immunoprecipitation and IP Kinase Assay

HEK293T cells were transfected with different plasmids for 48 h and HCT116 were seeded in 10 cm dishes for 24 h. Then, cells were harvested in IP buffer (50 mM tris-HCl pH 7.4, 150 mM NaCl, 1 mM EDTA, 1% NP40, and 1 mM DTT). 2 mg proteins were subjected to immunoprecipitation following the manufacturer's instructions. (Http://www.scbt.com/protocols.ht ml?protocol = immunoprecipitation). The mouse source antibody was used for IP and the rabbit source antibody was used for western blotting.

The BCKDK-Flag kinase was prepared with same method of Immunoprecipitation except BCKDK-Flag was diluted in 1× kinase buffer (Billerica, MA, USA) instead of 2× loading buffer (Santa Cruz, CA, USA). Likewise, MEK1 (residues 62-393)-his was prepared as above. 2 mg MEK1 (residues 62-393)-his was use for IP Kinase. The kinase and substrate were incubated at 37 °C for 70 min in 1× kinase buffer containing 100 μmol/L unlabeled ATP. If a kinase inhibitor was used, the kinase was first incubated with the inhibitor (0–3200 μM) at 32 °C for 20 min in 1× kinase buffer. The appropriate substrates were then added to the reactions and incubated at 37 °C for another 70 min. Samples were treated with 5× loading buffer and analyzed by western blotting.

2.7. Anchorage-independent Cell Transformation Assay

Different cell lines (8×10^3/well) were seeded in 6-well plates, and exposed or not exposed to EGF (20 ng/mL), BCAA (180–5670 μM) or inhibitor (0–3200 μM). The cells were then cultured in 1 mL of 0.33% BME (Eagle basal medium, Sigma-Aldrich Corp.) Agar (Sigma-Aldrich Corp.) containing 10% FBS, 2 mM L-glutamine, and 25 μg/mL gentamicin, with an additional 3 mL of 0.5% BME agar containing 10% FBS, 2 mM L-glutamine, and 25 μg/mL gentamicin being below. Then the cells were maintained in a 37 °C, 5% CO_2 incubator for 4–7 days and the colonies were observed and assessed by microscopy.

2.8. Tumor Xenografts and Immunohistochemistry

Male athymic Balb/c nude mice (4–6-week-old) were purchased from Beijing HFK Bioscience Co, Ltd. (Beijing, China). The mice were housed and maintained with the guide for care and use of laboratory animals which were approved by the Fourth Military Medical University. Mice were divided and randomized into two groups. Each of the different cell lines (3×10^6 in 200 μl PBS) was injected subcutaneously into the right flank. The tumor volumes were measured every other day and were calculated with the formula: V = 0.52 (length × width × height). The tumor tissues were prepared with paraffin sections after fixation with formalin, and then stained with hematoxylin and eosin (H&E) or p-MEK1/2(ser221) (1:50) and p-ERK1/2 (Tyr202/Tyr204) (1:50).

2.9. BCAA Assay and Tissue Microarray

The serums were obtained from the department of State Key Laboratory of Cancer Biology, Xijing hospital of the Fourth Military Medical University. The tissues used for BCAA assay and tissue microarray (TMA) underwent CRC were obtained from the department of Urology, Xijing hospital of the Fourth Military Medical University. This study was approved by the ethical committee of the Fourth Military Medical University. Samples were obtained with informed consent. The BCAA assay was following the manufacturer's instructions (http://www.sigmaaldrich.com/catalog/pro- duct/sigma/mak003?lang=en&region=GB). The TMA was stained with anti-BCKDHA, anti-BCKDK or anti-p-BCKDK antibody. The immuno-scores were calculated following the Remmele score method (Regitnig et al., 2002), and the scores > 3 were used as positive group, the others were used as negative group.

2.10. Statistical Analysis

All quantitative data in the present study were performed at least in triplicate. The results are expressed as the mean ± standard deviation. A two-tailed ANOVA or Student's *t*-test was used to evaluate the data, and $p < 0.05$ was considered significant (*$p < 0.05$, ** $p < 0.01$, ***$p < 0.001$).

3. Results

3.1. BCAA Cannot Promote CRC Tumorigenesis

BCAA is catabolized to R-CoA in normal cells. This process can be limited when BCKDH is phosphorylated by BCKDK at the Ser293 (Fig. S1a) (Chuang et al., 2002). The concentration of BCAA is higher in tumor tissues compared with normal tissues (Nezami Ranjbar et al., 2015). Metabolites can promote cell transformation directly (Liu et al., 2015; Nelson et al., 2013). Although the level of BCAA is higher in tumor, its role on cell transformation remains unrevealed. The JB6 C141 cell line represented a unique model for studying neoplastic transformation (Bernstein and Colburn, 1989); and therefore BCAA was added to JB6 C141 cells to assess its effect on anchorage-independent cell transformation. The result indicated that BCAA could not promote cell transformation, even at very high concentration (16 times higher than serum concentration, Fig. S1b) (Areces et al., 2015; Kooman et al., 1997; Szpetnar et al., 2014). Next, we detected the concentration of BCAA in the serums from 31 normal people and CRC patients or in the tissues from 10 CRC patients paired tumor and corresponding tumor adjacent tissues. The result showed that the concentration of BCAA had no significant change in CRC patient serums or tissues compared with normal people serums ($p = 0.837$) or adjacent tissues ($p = 0.661$) (Fig. S1c). Therefore, BCAA could not promote CRC tumorigenesis. It has been widely reported that BCAA catabolism is abnormal in cancer patients; especially BCAT1 plays an important role in glioma (Tönjes et al., 2013). However, there are two more key limiting enzymes, BCKDH and BCKDK in BCAA catabolism, and whether they are related to cancer, like BCAT1, has never been reported. Therefore, we decided to explore the role of BCKDH and BCKDK in CRC.

3.2. BCKDK Over-expression is Associated With Poor Prognosis in CRC Patients

Next, the expression levels of BCKDHA and BCKDK were analyzed in CRC tissue and corresponding tumor adjacent tissue samples. The results indicated that expression level of BCKDHA was higher in CRC tissue than that of corresponding tumor adjacent tissue samples from 117 cancer patients (Fig. 1a upper and middle panel), although, it had no effect on survival time ($p = 0.112$, Fig. 1a lower panel). The expression level of BCKDK was also higher in cancer tissue than adjacent tissue (Fig. 1b upper and middle panel), and it had a significant effect on survival time ($p = 0.011$, Fig. 1b lower panel). BCKDHA is the substrate of BCKDK, so next the expression levels of p-BCKDHA were assessed in the same way. While p-BCKDHA, was higher in cancer tissue than adjacent tissue (Fig. 1c upper and middle panel), it had no significant effect on survival time ($p = 0.368$, Fig. 1c lower panel). The above data suggest that BCKDK may be more important than BCKDHA in CRC patients. The higher level of BCKDK can result in higher level of BCAA; however, BCAA has no effect on cell transformation (Fig. S1b). Since BCAA catabolism is abnormal in cancer patients, BCKDK is one of the three

a

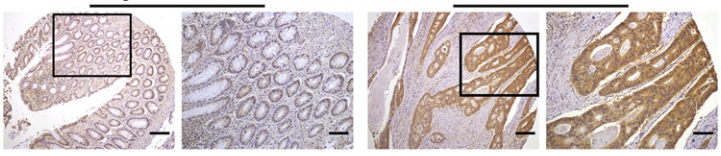

Group	BCKDHA expression +	-	P value
Adjacent tissue	12	79	< 0.001
Colorectal cancer tissue	58	59	

Survial Time (months)		
BCKDHA expression	Mean (95% CI)	P value
Positive	79 (68-90)	**0.112**
Negtive	92 (78-105)	

b

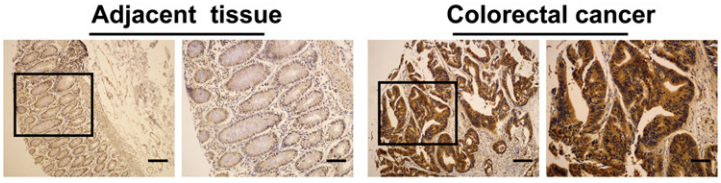

Group	BCKDK expression +	-	P value
Adjacent tissue	72	38	< 0.001
Colorectal cancer tissue	111	2	

Survial Time (months)		
BCKDK expression	Mean (95% CI)	P value
Positive	69 (54-84)	**0.011**
Negtive	94 (84-103)	

c

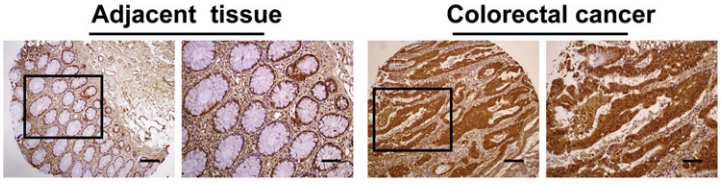

Group	p-BCKDHA expression +	-	P value
Adjacent tissue	15	82	< 0.001
Colorectal cancer tissue	65	53	

Survial Time (months)		
p-BCKDHA expression	Mean (95% CI)	P value
Positive	87 (78-97)	**0.368**
Negtive	75 (58-93)	

Fig. 1. BCKDK overexpression is associated with poor prognosis in CRC patients. (a) Immunohistochemical examination for the expression of BCKDHA in 117 cases of human colon cancer tissues and matching adjacent tissues. Pictures from 1 representative case are shown in the *upper panel*, and the 2 scale bars from left to right in each group correspond to 50 and 25 μm respectively. The table summarizes the results of the immunohistochemical examination (*middle panel*). The median survival time is no different between BCKDHA positive CRC patients and BCKDHA negative CRC patients (*lower panel*). The survival time table was analyzed *via* the Kaplan-Meier method. (b) Immunohistochemical examination for the expression of BCKDK in 113 cases of human colon cancer tissues and matching adjacent tissues. Pictures from 1 representative case are shown in the *upper panel*, and the 2 scale bars from left to right in each group correspond to 50 and 25 μm, respectively. The table summarizes the results of the immunohistochemical examination (*middle panel*). The median survival time is shorter for BCKDK-positive CRC patients than for BCKDK-negative CRC patients (*lower panel*). The survival time table was analyzed *via* the Kaplan-Meier method. (c) Immunohistochemical examination for the expression of p-BCKDHA in 118 cases of human colon cancer tissues and matching adjacent tissues. Pictures from 1 representative case are shown in the *upper panel*, and the 2 scale bars from left to right in each group correspond to 50 and 25 μm, respectively. The table summarizes the results of the immunohistochemical examination (*middle panel*). The median survival time is not different between p-BCKDHA-positive CRC patients and p-BCKDHA-negative CRC patients (*lower panel*). The survival time table was analyzed *via* the Kaplan-Meier method.

key molecules in BCAA catabolism (Fig. S1a), and there is no report about the role of BCKDK in cell transformation, we therefore further explored the possible role of BCKDK in CRC, described below.

3.3. BCKDK Promotes Tumorigenesis

First, BCKDK expression level was analyzed in 6 CRC cell lines and 1 normal intestinal epithelial cell line (Fig. 2a). The results showed that BCKDK was highly expressed in DLD1 and HCT116 cells, moderately expressed in HCT8 and HCT15 cells, and poorly expressed in SW480 and WiDr cells. The BCKDK level of normal HIEC-6 cells was the lowest. This result was consistent with that in CRC tissues from patients. To test whether BCKDK can promote cell transformation, BCKDK was next overexpressed in JB6 Cl41 cells or WiDr cells which poorly expressed BCKDK. JB6 Cl41 or WiDr stable cell lines that overexpressed the pCMV-c-Flag or pCMV-BCKDK-Flag were generated and the growth curves of JB6-Mock and JB6-BCKDK cells, or WiDr-Mock and WiDr-BCKDK cells were compared. The results showed that JB6-BCKDK cells grew faster than JB6-Mock cells (Fig. 2b upper left panel, inner session of left panel indicating BCKDK overexpression). Next, the anchorage-independent growth of JB6-Mock or JB6-BCKDK was compared, and the result indicated that the number of colonies in JB6-BCKDK cell cultures was much more than that in JB6-Mock cell cultures (Fig. 2b upper right panel). The corresponding statistical significance is shown in the right panel of Fig. 2b. Similar results were observed in the cultures of WiDr-Mock or WiDr-BCKDK stable cells (Fig. 2b lower panel). These results indicate that BCKDK promotes cell transformation. To verify this idea further, BCKDK was knocked down in HCT116 or DLD1 CRC cells to generate two stable shBCKDK cell lines and two stable shMock cell lines (HCT116-shBCKDK, HCT116-shMock or DLD1-shBCKDK, DLD1-shMock). As shown in Fig. 2c inner session of left panel by the result of Western blot, BCKDK was knocked down by shRNA sequence for lines 4 and 5. Next, growth curves of HCT116-shMock, -shBCKDK4, or -shBCKDK5 cells were tested, and the results demonstrated that HCT116-shBCKDK cells grew dramatically slower than HCT116-shMock cells ($p < 0.05$, Fig. 2c upper left panel). Next, the anchorage-independent growth of the HCT116-shMock or HCT116-shBCKDK cell lines was evaluated, and the results indicated that the number of colonies in HCT116-shBCKDK cell cultures was much less than in HCT116-shMock cell cultures (Fig. 2c upper right panel). Similar results were observed in the DLD1-shMock or DLD1-shBCKDK cell lines (Fig. 2c lower panels). Therefore, these results indicated that knockdown of BCKDK in colorectal tumor cells inhibited tumorigenesis *ex vivo*. Next, tumor xenograft assays were performed in male athymic Balb/c nude mice. We injected HCT116-shMock or HCT116-shBCKDK4 cells (3×10^6) subcutaneously into the right flank, with tumor size assessed over time. Tumors in HCT116-shMock-inoculated mice grew to a much larger size compared to those in HCT116-shBCKDK-inoculated mice (Fig. 2d left panel). The tumor growth curve is shown in the right panel of Fig. 2d. These data demonstrated that blocking BCKDK expression in CRC cells significantly reduces their tumorigenic properties *ex vivo* and *in vivo*, and further confirmed that BCKDK promotes cell transformation.

3.4. BCKDK Promotes Tumorigenesis Through Up-regulating the MEK-ERK Signaling Pathway

We confirmed that BCKDK promoted cell transformation *ex vivo* and *in vivo*. Next, we wanted to know which signaling pathway was involved in this process. The MAPK signaling pathway has been widely reported to link with carcinogenesis, with MEK and ERK being two critical kinases in this pathway (Rauch et al., 2016; Zhu et al., 2007). Therefore, p-MEK1/2 (ser221) and p-ERK1/2 (T202/Y204) levels were tested in JB6 Cl41 and WiDr BCKDK stable cell lines, and the results indicated that the level of p-MEK and p-ERK were up-regulated when BCKDK was overexpressed (Fig. 3a). These results suggest that BCKDK promotes CRC through up-regulating MEK-ERK activity. Next, the level of p-MEK and p-ERK were tested in the HCT116 or DLD1 shBCKDK cell lines. Both p-MEK and p-ERK were decreased significantly when BCKDK was knocked down in each of these cell lines (Fig. 3b). Next, the expression level of p-MEK1/2 (Ser221), p-ERK1/2(T202/Y204), and BCKDK were detected in tumor tissues dissected from the xenografts in the study by Western blotting or immunohistochemical analysis. The results confirmed that the level of p-MEK1/2 (Ser221), p-ERK1/2(T202/Y204), and BCKDK were higher in the tumor tissue of HCT116-shMock mice than in the tumor tissue of HCT116-shBCKDK mice (Fig. 3c). And the dissected tissues were also stained with hematoxylin & eosin (H&E) to confirm these tissues belong to tumor tissues (Fig. 3c right lower panel). These data confirmed that BCKDK promoted colorectal tumorigenesis through up-regulating the MEK-ERK signaling pathway.

3.5. BCKDK Directly Phosphorylates MEK1 at ser221

We elucidated that the levels of p-MEK1/2 (ser221) and p-ERK1/2 (T202/Y204) could be controlled by BCKDK, which implied that BCKDK might interact with MEK and phosphorylate it at Ser221 directly. First, whether BCKDK can interact with MEK was tested by co-immunoprecipitation experiments utilizing HEK293T cells. MEK1 and MEK2 share 79% amino acid similarity and are able to phosphorylate ERK substrates with equivalent capacity (Scholl et al., 2005). However, MEK1 plays a more important role in the growth and development of mice (Bélanger et al., 2003; Giroux et al., 1999). So pCMV-BCKDK-Flag or pCMV-Myc-MEK1 construct was transfected or co-transfected into HEK293T cells, then immunoprecipitated the tagged proteins with the Flag or Myc antibody, and then probed with anti-Flag or anti-Myc, respectively, in Western Blot assays. The results demonstrated that BCKDK could co-immunoprecipitate with MEK1 (Fig. 4a). However, since the detected interaction was performed in an overexpression system, we next assessed whether endogenous BCKDK was immunoprecipitated from HCT116 cells, as detected by Western blotting with a MEK antibody. The results indicated that BCKDK could co-immunoprecipitates with MEK1 in HCT116 cells (Fig. 4b). BCKDK is a protein kinase, so we next determined if it can phosphorylate MEK directly. An *in vitro* kinase assay was set up to test this idea. For this, we first obtained BCKDK by immunoprecipitation form overexpressing HEK293T cells and used it as the kinase. Inactive MEK1 (residues 62-393) was used as the substrate. The kinase assay was performed in the presence of cold ATP, with p-MEK1/2(Ser221) subsequently detected by Western blotting. The results indicated that BCKDK could phosphorylate MEK1 at Ser221 directly (Fig. 4c). Next, BCKDK was overexpressed in HEK293T cells, the cells were stimulated with EGF, and the endogenous phosphorylation of MEK was subsequently analyzed. These data indicated that increasing the amount of BCKDK leads to increased phosphorylation of endogenous MEK1/2 (Fig. 4d), further suggesting that BCKDK can phosphorylate MEK1/2 at Ser221 directly.

3.6. BCKDK Inhibitor Reduces Tumorigenic Properties

As shown above, BCKDK can promote tumorigenesis in CRC. Therefore, compounds may reduce tumorigenic properties if they can inhibit BCKDK. PB is an inhibitor of BCKDK which has been used to modulate BCAA catabolism (Tso et al., 2013). However, whether PB can block CRC is not known. Here, we used this inhibitor to further confirm the hypothesis that BCKDK promotes colorectal tumorigenesis *via* phosphorylating MEK1 at Ser221 and then activating the MEK-ERK signal pathway. First, MTS assays were performed to assess any potential cytotoxicity of this inhibitor in HCT116 cells that expressed a high level BCKDK. The results indicated that PB had no cytotoxicity in HCT116 cells at 48 h, even at a very high (3200 μM) concentration (Fig. 5a). Second, PB was used directly in *in vitro* kinase assays to test if it can inhibit p-MEK1 by reducing BCKDK activity. The results indicated that PB can inhibit the phosphorylation level of MEK1 at Ser221 in a dose dependent manner (Fig. 5b). Third, the expression of p-MEK1/2 (ser221), p-ERK1/2 (T202/Y204), and p-BCKDHA (Ser393) were detected in the HCT116 cells treated with different concentrations of PB. The results demonstrated that PB inhibited the level

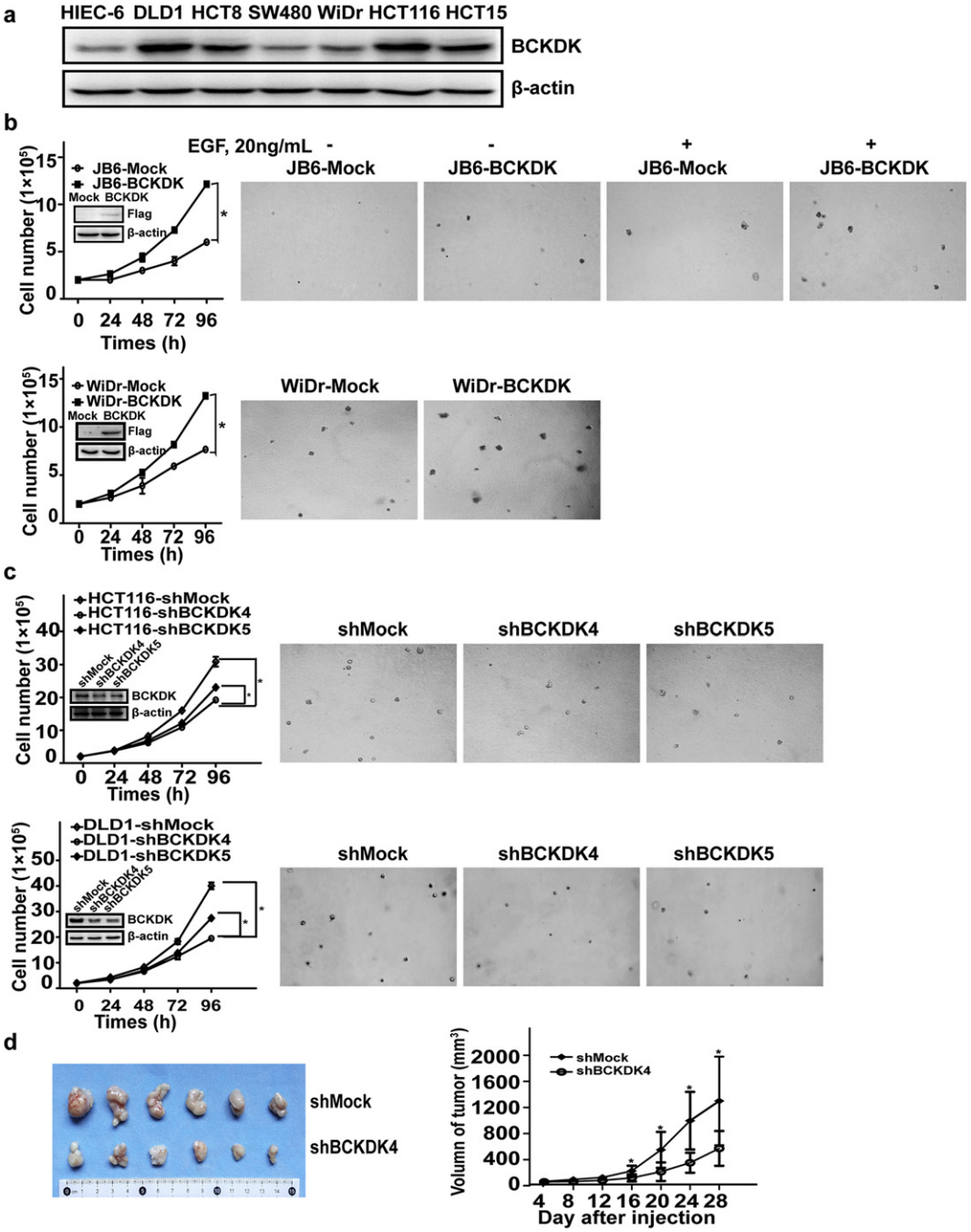

Fig. 2. BCKDK promotes tumorigenesis. (a) Expression of BCKDK in 7 different colorectal cell lines. (b) Growth curves of vector control cells (JB6-Mock) and BCKDK-overexpressing cells (JB6-BCKDK) (*upper left panel*). *Insert* shows verification of the cell lines identified by Western blot. Data are represented as mean ± standard deviation from triplicate experiments. The asterisk indicates a significant increase in cell number in JB6-BCKDK cells compared with JB6-Mock cells (*, $P < 0.05$). BCKDK can transform JB6 C141 cells *ex vivo* as illustrated by growth of BCKDK-transformed cells in soft agar. Photomicrograph of representative colony formation in soft agar of vector control cells (JB6-Mock) compared with BCKDK-overexpression cells (JB6-BCKDK) is shown (*upper right panel*). Growth curves of vector control cells (WiDr-Mock) and BCKDK-overexpressing cells (WiDr-BCKDK) (*lower left panel*). *Insert* shows verification of the cell lines identified by Western blot. Data are represented as mean ± standard deviation from triplicate experiments. The asterisk indicates a significant increase in cell number in WiDr-BCKDK cells compared with WiDr-Mock cells (*, $P < 0.05$). BCKDK can enhance the transformation of WiDr cells *ex vivo* as illustrated by growth of BCKDK transformed cells in soft agar. Photomicrograph of representative colony formation in soft agar of vector control cells (WiDr-Mock) compared with BCKDK-overexpressing cells (WiDr-BCKDK) is shown (*lower right panel*). (c) Growth curves of HCT116/DLD1-shMock, HCT116/DLD1-shBCKDK4, and HCT116/DLD1-shBCKDK5 cells (*left panel*). *Insert* shows verification of the knockdown cell lines identified by Western blot. Data are represented as mean ± standard deviation from triplicate experiments. The asterisks indicate a significant increase compared with shMock cells (*, $P < 0.05$). Knockdown of BCKDK reduces tumorigenic properties of HCT116/DLD1 CRC cells *ex vivo*. Representative photomicrograph of colony formation in soft agar of vector control cells (shMock) compared with BCKDK-knockdown cells (shBCKDK4 or shBCKDK5) is shown (*right panel*). Data are represented as mean ± standard deviation from triplicate experiments (*right panel*). (d) Knockdown of BCKDK reduces tumorigenic properties of HCT116 CRC cells *in vivo*. Tumors dissected from each group are shown (*left panel*). Final average tumor growth curve of mice injected with HCT116-shMock or HCT116-shBCKDK cells is shown (*right panel*). Data are shown as means ± standard deviation of measurements. The asterisk indicates a significant decrease in tumor size in HCT116-shBCKDK4-injected mice compared with HCT116-shMock-injected mice (*, $P < 0.05$). All Western blot data are representatives of results from triplicate experiments.

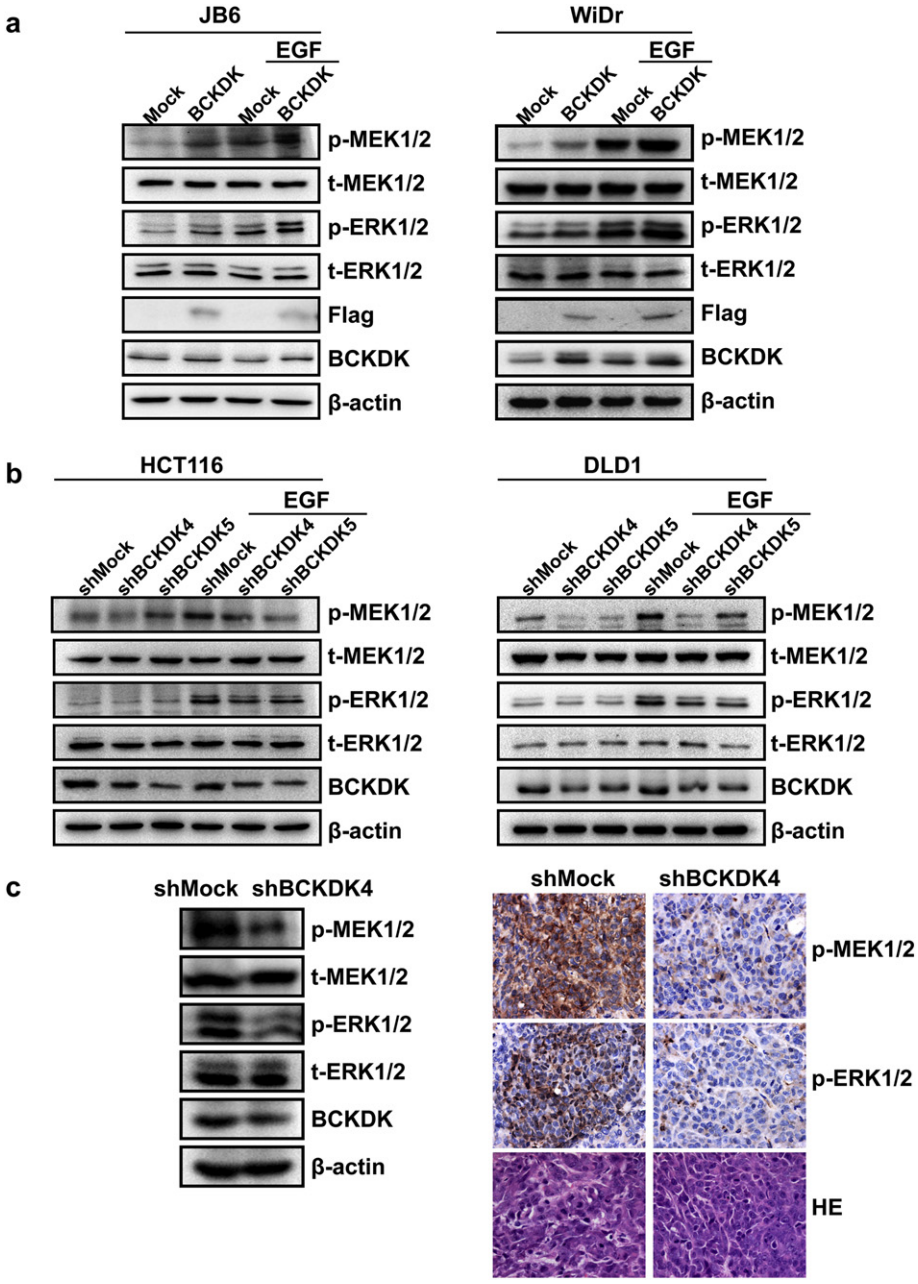

Fig. 3. BCKDK promotes tumorigenesis through up-regulating MEK-ERK signaling pathway. (a) The level of phosphorylation of MEKs and ERKs were increased in JB6/WiDr-BCKDK cells after EGF treatment for 15 min. (b) The level of phosphorylation of MEKs and ERKs were decreased in HCT116/DLD1-shBCKDK cells after EGF treatment for 15 min. (c) The level of phosphorylation of MEKs and ERKs were decreased in the tumor tissues from HCT116-shBCKDK4-injected mice compared to HCT116-shMock-injected mice (*left panel*). Immunohistochemistry analysis was performed in the tumor tissues of HCT116-shMock-injected mice or HCT116-shBCKDK4-injected mice (*right panel*). All Western blot data are representatives of results from triplicate experiments.

of p-MEK1/2 (ser221), p-ERK1/2 (T202/Y204), or p-BCKDHA at 200 μM and 800 μM (Fig. 5c). Last, soft agar assays were used to test if PB could block anchorage-independent growth of HCT116 cells. The data indicated that PB inhibited anchorage-independent growth of HCT116 cells from the concentration of 800 μM, and corresponding statistical significance was showed in the lower right panel (Fig. 5d).

Taken together, our study indicates that BCKDK promotes colorectal tumorigenesis through up-regulation of the MAPK signaling pathway by phosphorylating MEK at Ser221.

4. Discussion

CRC is the fourth most common cause of cancer deaths, with 600,000 deaths is reported in the world annually (Torre et al., 2015). Significant progress has been achieved in understanding the molecular pathways involved in the carcinogenesis of CRC during the past three decades, which brings great benefits to CRC patients by targeted drugs (He et al., 2016; Kuo et al., 2016; Manchado et al., 2016; van der Velden et al., 2016). As the effectiveness of those targeted drugs is limited by intrinsic drug resistance (Tong et al., 2017; Zhang et al., 2016), there are some patients who are remaining "undruggable". About 40% of CRC patients with wild type EGFR, KRAS, or BRAF are still resistant to anti-EGFR treatment (Bardelli and Siena, 2010; De Roock et al., 2010; Douillard et al., 2013). MEK has unique characteristics among the components of the MAPK pathways and has been considered as an ideal therapeutic target, because it can integrate many mitogenic signals into the ERKs, its only substrates. The expression level of MEK is higher in renal cell carcinoma resistant tissues than in renal cell carcinoma tissue when treated with

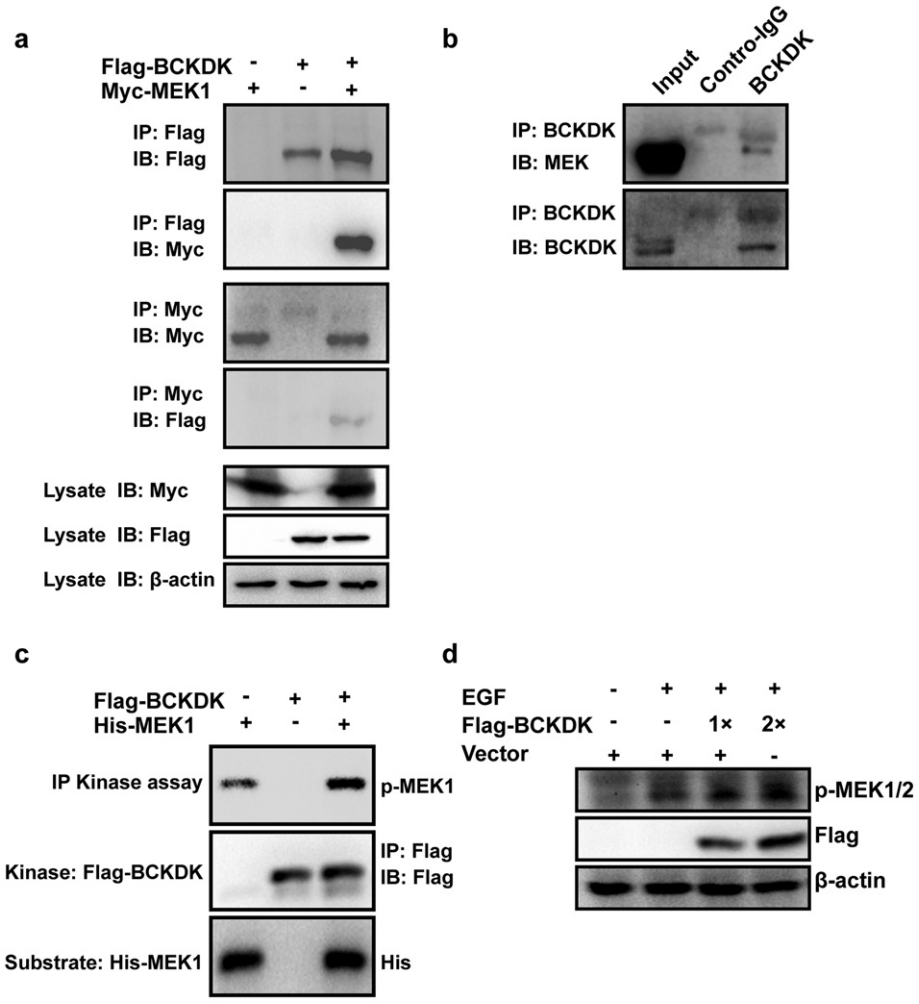

Fig. 4. BCKDK directly phosphorylates MEK1 at ser221. (a) BCKDK binds with MEK in HEK 293 T cells after transient transfection as indicated. pCMV-Flag-BCKDK or pCMV-Myc-MEK1 construct was trasfected or co-transfected into HEK 293T cells, immunoprecipitated with an anti-Flag or anti-Myc antibody, and then probed with Flag or anti-Myc antibody, respectively. (b) BCKDK binds with MEK in HCT116 cells. Endogenous BCKDK was immunoprecipitated from HCT116 cells and then probed with anti-MEK antibody. (c) BCKDK phosphorylates MEK1 *in vitro*. The samples in A were subjected to immunoprecipitation using the mouse source Flag antibody, and then a kinase assay was performed with His-MEK1(residues 62-393) as substrate, and corresponding rabbit source antibodies were used in Western blot analyses. (d) BCKDK promotes phosphorylation of endogenous MEK in HEK 293 T cells in a dose-dependent manner after EGF treatment for 15 min. Increasing amounts of Flag-BCKDK were transiently transfected into HEK 293 T cells, and the level of phosphorylation of MEKs was detected by Western blot. All Western blot data are representatives of results from triplicate experiments.

tyrosine kinase inhibitors (TKIs) (Li et al., 2015; Qin et al., 2016), suggesting an alternative activation signaling pathway of MEK may exist besides the RAF-MEK pathway, and therefore contribute to drug resistance. MEK is a downstream key kinase of the EGFR signaling pathway and is a potential therapeutical target (McCubrey et al., 2010). In our research, BCKDK was demonstrated as an upstream kinase of MEK, phosphorylating MEK at serine 221 (Fig. 4). Therefore, blocking the BCKDK-MEK signaling pathway might be a potential therapeutic strategy for CRC.

PB is a well-known BCKDK inhibitor which can inhibit phosphorylation of BCKDHA. It also acts as a histone deacetylase inhibitor (Lea and Tulsyan, 1995) which had been shown to inhibit tumor growth in a wide variety of cancer cell lines, such as, colorectal cancer, glioblastoma, prostate cancer, and melanoma (Huang et al., 2000; Kusaczuk et al., 2016; Carducci et al., 1996; Liu et al., 1994). Furthermore, Sung and Waxman (2007) demonstrated that Weekly infusions of PB combined with FUra were fairly well tolerated with disease stabilization in 3/4 (75%) of colorectal cancer patients. However, Brinkmann et al. (2001) showed that hyperacetylated histones accumulation induced by histone deacetylase inhibitors was not sufficient to cause growth inhibition in all cell types. And the dose limiting neurocortical toxicity of confusion and excessive somnolence occurred in the patients of colorectal cancer, glioblastoma or prostate cancer who were treated with PB (Sung and Waxman, 2007; Kusaczuk et al., 2016; Carducci et al., 2001). High concentrations of PB are required to block BCKDK activity *ex vivo* (Brunetti-Pierri et al., 2011) or *in vivo* (Fig. 5b). Therefore, more efficient inhibitors than PB for targeting BCKDK should be identified to overcome drug resistance of CRC caused by consistent MEK activation.

Many biomarkers have been used for CRC screening. Stool-Based Biomarker, Hemoglobin is widely used despite the low specificity (80%–90%) and relatively low sensitivity (30%–50%) of this assay for the detection of advanced polyps and cancers (Zhu et al., 2010). Other types of fecal biomarkers, such as DNA biomarkers, have also been extensively tested and approved for clinical use, including the chromosomal instability pathway (CIN), the microsatellite instability (MSI) pathway, and the serrated polyp or CpG island methylator phenotype (CIMP) pathway. APC, EGFR, KRAS, BRAF, TP53, PIK3CA, ERBB2 detection have likewise been used in CRC screening (Dickinson et al., 2015). Our data shows that BCKDK is expressed at higher levels in colorectal tissues *versus* adjacent normal tissues, and patients who have higher BCKDK immuno-scores in their local focus tissues have a shorter survival time (Fig. 1b). This suggests that BCKDK can be another potential and valuable biomarker for the diagnosis of CRC.

BCAA level increases when BCKDK is over-expressed (Chuang et al., 2004; García-Cazorla et al., 2014; Nellis et al., 2003), but the role of

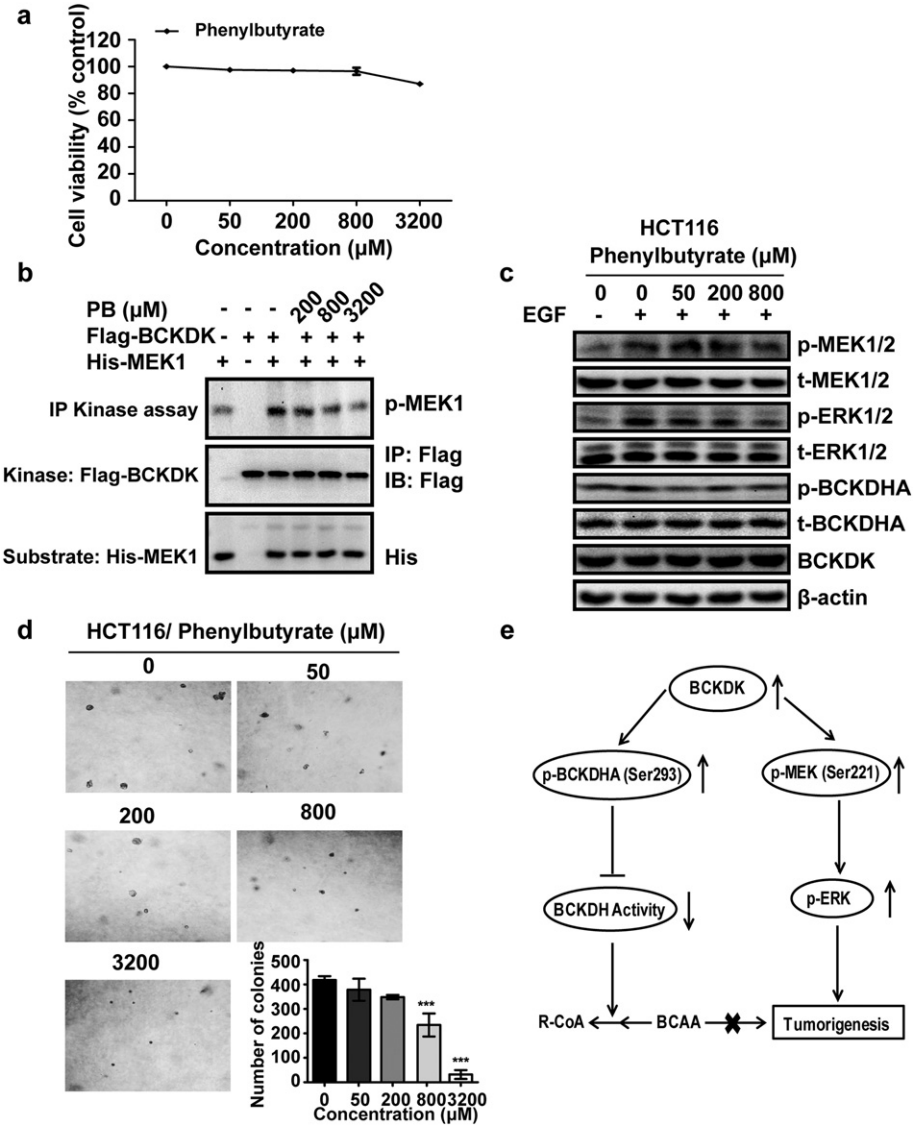

Fig. 5. BCKDK inhibitor, Phenyl butyrate (PB) reduces tumorigenic properties. (a) Cytotoxic effects of PB on HCT116 cells. An MTS assay was used after treatment of HCT116 cells with PB for 48 h. The experiments were performed in triplicate, and the mean absorbance was calculated. (b) PB inhibits the phosphorylation of MEK by BCKDK. The samples in Fig. 4A were subjected to immunoprecipitation using the mouse source Flag antibody, and BCKDK was pre-incubated with PB at 32 °C for 20 min firstly, followed by kinase assays with His-MEK1 (residues 62-393) as substrate, and then corresponding rabbit source antibodies used to detect the level of MEK1 phosphorylation by Western blot. (c) HCT116 cells were treated with PB for 48 h in a dose-dependent manner. The cells were then lysed and analyzed by Western blot. (d) PB inhibits BCKDK-induced anchorage-independent growth of HCT116 cells. Data are shown as means ± standard deviation of values from three independent experiments (*right lower panel*). The asterisks indicate a significant decrease in colony formation in cells treated with PB compared with the non-treated cells (***, $P < 0.001$). (e) Schematic diagram showing the mechanism of BCKDK in CRC. All Western blot data are representatives of results from triplicate experiments.

BCAA in colorectal tumorigenesis or cancer growth has remained undetermined, whether the concentration of BCAA in CRC patient serums or tumor tissues is also higher compared with the normal people serums or adjacent tissues is still unknown. First, our data indicated that BCAA could not promote cell transformation directly (Fig. S1b). Second, the concentration of BCAA has no significant change in CRC patient serums or tumor tissues compared with the normal people serums or adjacent tissues (Fig. S1c). BCAA in cancer (three essential amino acids) may be used for protein synthesis (Chiarla et al., 1997). In summary, BCAA could not promote CRC tumorigenesis, and these three essential amino acids might provide raw materials for biosynthesis to maintain tumor cells' growth and survival (Fig. 5e).

Taken together, our data revealed that BCKDK is highly expressed in CRC tissue, may be a valuable biomarker for CRC, and may promote transformation or oncogenesis by phosphorylating MEK directly at Ser221 (Fig. 5e) rather than through BCAA catabolism. Crosstalk between BCKDK and MEK may therefore serve as therapeutic target to overcome drug resistance of CRC.

Funding Sources

This project was supported by the National Natural Science Foundation of China (nos. 81672936, 81672739, & 81472602) and, the Independent Innovation Project of Huazhong University of Science and Technology (nos. 2016YXZD034, 2014TS063, 2015QN151 & 2014ZZGH013), and the State Key Laboratory of Cancer Biology Foundation (no. CBSKL2014Z18).

Conflict of Interest

The authors have no conflict of interest.

Author Contributions

Peipei Xue, Juanjuan Xiao, Linni Fan, Huimin Sun, Malyarenko Olesya, and Jianmin Zhang were involved in the acquisition of experimental data. Wei Yan and Zhe Wang performed the tissue microarray analysis. Shaoqing Liu analyzed the clinical data. Jianyong Zheng and Zhe Wang provided the clinical samples. Chen Shao provided the mice. Lin Liu, Ping Yuan, Hui Lu, and Ruijuan Xiu provided advice on the manuscript. Peipei Xue, Fanfan Zeng, Qiuhong Duan and Feng Zhu designed the study, analyzed the data and drafted the manuscript.

Appendix A. Supplementary data

Supplementary data to this article can be found online at http://dx.doi.org/10.1016/j.ebiom.2017.05.001.

References

Areces, F., González-Millán, C., Salinero, J.J., Abian-Vicen, J., Lara, B., Gallo-Salazar, C., Ruiz-Vicente, D., Del Coso, J., 2015. Changes in serum free amino acids and muscle fatigue experienced during a half-ironman triathlon. PLoS One 10, e0138376.

Bardelli, A., Siena, S., 2010. Molecular mechanisms of resistance to cetuximab and panitumumab in colorectal cancer. J. Clin. Oncol. 28, 1254–1261.

Beaudet, A.L., 2012. Neuroscience. Preventable forms of autism? Science 338, 342–343.

Bélanger, L.F., Roy, S., Tremblay, M., Brott, B., Steff, A.M., Mourad, W., Hugo, P., Erikson, R., Charron, J., 2003. Mek2 is dispensable for mouse growth and development. Mol. Cell. Biol. 23, 4778–4787.

Bernstein, L.R., Colburn, N.H., 1989. AP1/jun function is differentially induced in promotion-sensitive and resistant JB6 cells. Science 244, 566–569.

Billingsley, K.L., Park, J.M., Josan, S., Hurd, R., Mayer, D., Spielman-Sun, E., Nishimura, D.G., Brooks, J.D., Spielman, D., 2014. The feasibility of assessing branched-chain amino acid metabolism in cellular models of prostate cancer with hyperpolarized [1-(13) C]-ketoisocaproate. Magn. Reson. Imaging 32, 791–795.

de Bont, J.M., Kros, J.M., Passier, M.M., Reddingius, R.E., Sillevis Smitt, P.A., Luider, T.M., den Boer, M.L., Pieters, R., 2008. Differential expression and prognostic significance of SOX genes in pediatric medulloblastoma and ependymoma identified by microarray analysis. Neuro-Oncology 10, 648–660.

Bradford, M.M., 1976. A rapid and sensitive method for the quantization of microgram quantities of protein utilizing the principle of protein-dye binding. Anal. Biochem. 72, 248–254.

Brinkmann, H., Dahler, A.L., Popa, C., Serewko, M.M., Parsons, P.G., Gabrielli, B.G., Burgess, A.J., Saunders, N.A., 2001. Histone hyperacetylation induced by histone deacetylase inhibitors is not sufficient to cause growth inhibition in human dermal fibroblasts. J. Biol. Chem. 276, 22491–22499.

Brunetti-Pierri, N., Lanpher, B., Erez, A., Ananieva, E.A., Islam, M., Marini, J.C., Sun, Q., Yu, C., Hegde, M., Li, J., Wynn, R.M., Chuang, D.T., Hutson, S., Lee, B., 2011. Phenylbutyrate therapy for maple syrup urine disease. Hum. Mol. Genet. 20, 631–640.

Burrage, L.C., Nagamani, S.C., Campeau, P.M., Lee, B.H., 2014. Branched-chain amino acid metabolism: from rare Mendelian diseases to more common disorders. Hum. Mol. Genet. 23, R1–R8.

Carducci, M.A., Nelson, J.B., Chan-Tack, K.M., Ayyagari, S.R., Sweatt, W.H., Campbell, P.A., Nelson, W.G., Simons, J.W., 1996. Phenyl-butyrate induces apoptosis in human prostate cancer and is more potent than phenylacetate. Clin. Cancer Res. 2, 379–387.

Carducci, M.A., Gilbert, J., Bowling, M.K., Noe, D., Eisenberger, M.A., Sinibaldi, V., Zabelina, Y., Chen, T.L., Grochow, L.B., Donehower, R.C., 2001. A Phase I clinical and pharmacological evaluation of sodium phenylbutyrate on an 120-h infusion schedule. Clin. Cancer Res. 7, 3047–3055.

Chiarla, C., Giovannini, I., Boldrini, G., Castagneto, M., 1997. The branched-chain amino acids. Minerva Gastroenterol. Dietol. 43, 189–196.

Chuang, J.L., Wynn, R.M., Chuang, D.T., 2002. The C-terminal hinge region of lipoic acid-bearing domain of E2b is essential for domain interaction with branched-chain alpha-keto acid dehydrogenase kinase. J. Biol. Chem. 277, 36905–36908.

Chuang, J.L., Wynn, R.M., Moss, C.C., Song, J.L., Li, J., Awad, N., Mandel, H., Chuang, D.T., 2004. Structural and biochemical basis for novel mutations in homozygous Israeli maple syrup urine disease patients: a proposed mechanism for the thiamin-responsive phenotype. J. Biol. Chem. 279, 17792–17800.

Conway, M.E., Hull, J., El Hindy, M., Taylor, S.C., El Amraoui, F., Paton-Thomas, C., White, P., Williams, M., Ellis, H.P., Bertoni, A., Radlwimmer, B., Hutson, S.M., Kurian, K.M., 2016. Decreased expression of the mitochondrial BCAT protein correlates with improved patient survival in IDH-WT gliomas. Brain Pathol. 26, 789–791.

De Roock, W., Claes, B., Bernasconi, D., De Schutter, J., Biesmans, B., Fountzilas, G., Kalogeras, K.T., Kotoula, V., Papamichael, D., Laurent-Puig, P., Penault-Llorca, F., Rougier, P., Vincenzi, B., Santini, D., Tonini, G., Cappuzzo, F., Frattini, M., Molinari, F., Saletti, P., De Dosso, S., Martini, M., Bardelli, A., Siena, S., Sartore-Bianchi, A., Tabernero, J., Macarulla, T., Di Fiore, F., Gangloff, A.O., Ciardiello, F., Pfeiffer, P., Qvortrup, C., Hansen, T.P., Van Cutsem, E., Piessevaux, H., Lambrechts, D., Delorenzi, M., Tejpar, S., 2010. Effects of KRAS, BRAF, NRAS, and PIK3CA mutations on the efficacy of cetuximab plus chemotherapy in chemotherapy-refractory metastatic colorectal cancer: a retrospective consortium analysis. Lancet Oncol. 11, 753–762.

Dickinson, B.T., Kisiel, J., Ahlquist, D.A., Grady, W.M., 2015. Molecular markers for colorectal cancer screening. Gut 64, 1485–1494.

Douillard, J.Y., Oliner, K.S., Siena, S., Tabernero, J., Burkes, R., Barugel, M., Humblet, Y., Bodoky, G., Cunningham, D., Jassem, J., Rivera, F., Kocákova, I., Ruff, P., Błasińska-Morawiec, M., Šmakal, M., Canon, J.L., Rother, M., Williams, R., Rong, A., Wiezorek, J., Sidhu, R., Patterson, S.D., 2013. Panitumumab-FOLFOX4 treatment and RAS mutations in colorectal cancer. N. Engl. J. Med. 369, 1023–1034.

García-Cazorla, A., Oyarzabal, A., Fort, J., Robles, C., Castejón, E., Ruiz-Sala, P., Bodoy, S., Merinero, B., Lopez-Sala, A., Dopazo, J., Nunes, V., Ugarte, M., Artuch, R., Palacín, M., Rodríguez-Pombo, P., Alcaide, P., Navarrete, R., Sanz, P., Font-Llitjós, M., Vilaseca, M.A., Ormaizabal, A., Pristoupilova, A., Agulló, S.B., 2014. Two novel mutations in the BCKDK (branched-chain keto-acid dehydrogenase kinase) gene are responsible for a neurobehavioral deficit in two pediatric unrelated patients. Hum. Mutat. 35, 470–477.

Gill, K.S., Fernandes, P., O'Donovan, T.R., McKenna, S.L., Doddakula, K.K., Power, D.G., Soden, D.M., Forde, P.F., 2016. Glycolysis inhibition as a cancer treatment and its role in an anti-tumour immune response. Biochim. Biophys. Acta 1866, 87–105.

Giroux, S., Tremblay, M., Bernard, D., Cardin-Girard, J.F., Aubry, S., Larouche, L., Rousseau, S., Huot, J., Landry, J., Jeannotte, L., Charron, J., 1999. Embryonic death of Mek1-deficient mice reveals a role for this kinase in angiogenesis in the labyrinthine region of the placenta. Curr. Biol. 9, 369–372.

He, E.Y., Wyld, L., Sloane, M.A., Canfell, K., Ward, R.L., 2016. The molecular characteristics of colonic neoplasms in serrated polyposis: a systematic review and meta-analysis. J. Pathol. Clin. Res. 2, 127–137.

Huang, Y., Horvath, C.M., Waxman, S., 2000. Regrowth of 5-fluorouracil-treated human colon cancer cells is prevented by the combination of interferon gamma, indomethacin, and phenylbutyrate. Cancer Res. 60, 3200–3206.

Hunter, T., Karin, M., 1992. The regulation of transcription by phosphorylation. Cell 70, 375–387.

Kooman, J.P., Deutz, N.E., Zijlmans, P., van den Wall Bake, A., Gerlag, P.G., van Hooff, J.P., Leunissen, K.M., 1997. The influence of bicarbonate supplementation on plasma levels of branched-chain amino acids in haemodialysis patients with metabolic acidosis. Nephrol. Dial. Transplant. 12, 2397–2401.

Kuo, W.T., Lee, T.C., Yu, L.C., 2016. Eritoran suppresses colon cancer by altering a functional balance in toll-like receptors that bind lipopolysaccharide. Cancer Res. 76, 4684–4695.

Kusaczuk, M., Krętowski, R., Bartoszewicz, M., Cechowska-Pasko, M., 2016. Phenylbutyrate-a pan-HDAC inhibitor-suppresses proliferation of glioblastoma LN-229 cell line. Tumour Biol. 37, 931–942.

Lea, M.A., Tulsyan, N., 1995. Discordant effects of butyrate analogues on erythroleukemia cell proliferation, differentiation and histone deacetylase. Anticancer Res. 15, 879–883.

Li, X.L., Chen, X.Q., Zhang, M.N., Chen, N., Nie, L., Xu, M., Gong, J., Shen, P.F., Su, Z.Z., Weng, X., Tan, J.Y., Zhao, T., Zeng, H., Zhou, Q., 2015. SOX9 was involved in TKIs resistance in renal cell carcinoma via Raf/MEK/ERK signaling pathway. Int. J. Clin. Exp. Pathol. 8, 3871–3881.

Liu, L., Shack, S., Stetler-Stevenson, W.G., Hudgins, W.R., Samid, D., 1994. Differentiation of cultured human melanoma cells induced by the aromatic fatty acids phenylacetate and phenylbutyrate. J. Invest Dermatol. 103, 335–340.

Liu, W., Hancock, C.N., Fischer, J.W., Harman, M., Phang, J.M., 2015. Proline biosynthesis augments tumor cell growth and aerobic glycolysis: involvement of pyridine nucleotides. Sci. Rep. 5, 17206.

Manchado, E., Weissmueller, S., Morris, J.P., Chen, C.C., Wullenkord, R., Lujambio, A., de Stanchina, E., Poirier, J.T., Gainor, J.F., Corcoran, R.B., Engelman, J.A., Rudin, C.M., Rosen, N., Lowe, S.W., 2016. A combinatorial strategy for treating KRAS-mutant lung cancer. Nature 534 (7609):647–651. http://dx.doi.org/10.1038/nature18600.

McCubrey, J.A., Steelman, L.S., Abrams, S.L., Chappell, W.H., Russo, S., Ove, R., Milella, M., Tafuri, A., Lunghi, P., Bonati, A., Stivala, F., Nicoletti, F., Libra, M., Martelli, A.M., Montalto, G., Cervello, M., 2010. Emerging MEK inhibitors. Expert Opin. Emerg. Drugs 15, 203–223.

Mitchell, S.M., Ross, J.P., Drew, H.R., Ho, T., Brown, G.S., Saunders, N.F., Duesing, K.R., Buckley, M.J., Dunne, R., Beetson, I., Rand, K.N., McEvoy, A., Thomas, M.L., Baker, R.T., Wattchow, D.A., Young, G.P., Lockett, T.J., Pedersen, S.K., Lapointe, L.C., Molloy, P.L., 2014. A panel of genes methylated with high frequency in colorectal cancer. BMC Cancer 14, 54.

Mochel, F., Charles, P., Seguin, F., Barritault, J., Coussieu, C., Perin, L., Le Bouc, Y., Gervais, C., Carcelain, G., Vassault, A., Feingold, J., Rabier, D., Durr, A., 2007. Early energy deficit in Huntington disease: identification of a plasma biomarker traceable during disease progression. PLoS One 2, e647.

Moffat, J., Grueneberg, D.A., Yang, X., Kim, S.Y., Kloepfer, A.M., Hinkle, G., Piqani, B., Eisenhaure, T.M., Luo, B., Grenier, J.K., Carpenter, A.E., Foo, S.Y., Stewart, S.A., Stockwell, B.R., Hacohen, N., Hahn, W.C., Lander, E.S., Sabatini, D.M., Root, D.E., 2006. A lentiviral RNAi library for human and mouse genes applied to an arrayed viral high-content screen. Cell 124, 1283–1298.

Nellis, M.M., Kasinski, A., Carlson, M., Allen, R., Schaefer, A.M., Schwartz, E.M., Danner, D.J., 2003. Relationship of causative genetic mutations in maple syrup urine disease with their clinical expression. Mol. Genet. Metab. 80, 189–195.

Nelson, E.R., Wardell, S.E., Jasper, J.S., Park, S., Suchindran, S., Howe, M.K., Carver, N.J., Pillai, R.V., Sullivan, P.M., Sondhi, V., Umetani, M., Geradts, J., McDonnell, D.P., 2013. 27-Hydroxycholesterol links hypercholesterolemia and breast cancer pathophysiology. Science 342, 1094–1098.

Nezami Ranjbar, M.R., Luo, Y., Di Poto, C., Varghese, R.S., Ferrarini, A., Zhang, C., Sarhan, N.I., Soliman, H., Tadesse, M.G., Ziada, D.H., Roy, R., Ressom, H.W., 2015. GC-MS based plasma metabolomics for identification of candidate biomarkers for hepatocellular carcinoma in Egyptian cohort. PLoS One 10, e0127299.

Novarino, G., El-Fishawy, P., Kayserili, H., Meguid, N.A., Scott, E.M., Schroth, J., Silhavy, J.L., Kara, M., Khalil, R.O., Ben-Omran, T., Ercan-Sencicek, A.G., Hashish, A.F., Sanders, S.J., Gupta, A.R., Hashem, H.S., Matern, D., Gabriel, S., Sweetman, L., Rahimi, Y., Harris,

R.A., State, M.W., Gleeson, J.G., 2012. Mutations in BCKD-kinase lead to a potentially treatable form of autism with epilepsy. Science 338, 394–397.
Pike, L.S., Smift, A.L., Croteau, N.J., Ferrick, D.A., Wu, M., 2011. Inhibition of fatty acid oxidation by etomoxir impairs NADPH production and increases reactive oxygen species resulting in ATP depletion and cell death in human glioblastoma cells. Biochim. Biophys. Acta 1807, 726–734.
Qin, C.P., Liu, C.L., Zhao, Y.H., Yin, H.Q., DU, Y.Q., Hu, F.Z., Sheng, Z.Z., Xu, T., 2016. Expression of MEK/ERK signal pathways in renal cell carcinoma with bone metastasis. Beijing Da Xue Xue Bao 48, 590–593.
Rauch, N., Rukhlenko, O.S., Kolch, W., Kholodenko, B.N., 2016. MAPK kinase signalling dynamics regulate cell fate decisions and drug resistance. Curr. Opin. Struct. Biol. 41, 151–158.
Regitnig, P., Reiner, A., Dinges, H.P., Höfler, G., Müller-Holzner, E., Lax, S.F., Obrist, P., Rudas, M., Quehenberger, F., 2002. Quality assurance for detection of estrogen and progesterone receptors by immunohistochemistry in Austrian pathology laboratories. Virchows Arch. 441, 328–334.
Sachsenmaier, C., Radler-Pohl, A., Zinck, R., Nordheim, A., Herrlich, P., Rahmsdorf, H.J., 1994. Involvement of growth factor receptors in the mammalian UVC response. Cell 78, 963–972.
Sassone-Corsi, P., Mizzen, C.A., Cheung, P., Crosio, C., Monaco, L., Jacquot, S., Hanauer, A., Allis, C.D., 1999. Requirement of Rsk-2 for epidermal growth factor-activated phosphorylation of histone H3. Science 285, 886–891.
Scafidi, J., Hammond, T.R., Scafidi, S., Ritter, J., Jablonska, B., Roncal, M., Szigeti-Buck, K., Coman, D., Huang, Y., McCarter Jr., R.J., Hyder, F., Horvath, T.L., Gallo, V., 2014. Intranasal epidermal growth factor treatment rescues neonatal brain injury. Nature 506, 230–234.
Scholl, F.A., Dumesic, P.A., Khavari, P.A., 2005. Effects of active MEK1 expression in vivo. Cancer Lett. 230, 1–5.
Sonnet, Davis S., O'Leary, M.N., Gutierrez, A.M., Nguyen, M.S., Mateen, S., Hsu, Y., Mitchell, P.K., Lopez, J.A., Vockley, J., Kennedy, K.B., Ramanathan, A., 2016. Metformin inhibits Branched Chain Amino Acid (BCAA) derived ketoacidosis and promotes metabolic homeostasis in MSUD. Sci. Rep. 6, 28775.
Sung, M.W., Waxman, S., 2007. Combination of cytotoxic-differentiation therapy with 5-fluorouracil and phenylbutyrate in patients with advanced colorectal cancer. Anticancer Res. 27, 995–1001.
Szpetnar, M., Matras, P., Boguszewska-Czubara, A., Kiełczykowska, M., Rudzki, S., Musik, I., 2014. Is additional enrichment of diet in branched-chain amino acids or glutamine beneficial for patients receiving total parenteral nutrition after gastrointestinal cancer surgery? Adv. Clin. Exp. Med. 23, 423–431.
Tong, J., Tan, S., Zou, F., Yu, J., Zhang, L., 2017. FBW7 mutations mediate resistance of colorectal cancer to targeted therapies by blocking Mcl-1 degradation. Oncogene 36, 787–796.
Tönjes, M., Barbus, S., Park, Y.J., Wang, W., Schlotter, M., Lindroth, A.M., Pleier, S.V., Bai, A.H., Karra, D., Piro, R.M., Felsberg, J., Addington, A., Lemke, D., Weibrecht, I., Hovestadt, V., Rolli, C.G., Campos, B., Turcan, S., Sturm, D., Witt, H., Chan, T.A., Herold-Mende, C., Kemkemer, R., König, R., Schmidt, K., Hull, W.E., Pfister, S.M., Jugold, M., Hutson, S.M., Plass, C., Okun, J.G., Reifenberger, G., Lichter, P., Radlwimmer, B., 2013. BCAT1 promotes cell proliferation through amino acid catabolism in gliomas carrying wild-type IDH1. Nat. Med. 19, 901–908.
Torre, L.A., Bray, F., Siegel, R.L., Ferlay, J., Lortet-Tieulent, J., Jemal, A., 2015. Global cancer statistics 2012. CA Cancer J. Clin. 65, 87–108.
Tso, S.C., Qi, X., Gui, W.J., Chuang, J.L., Morlock, L.K., Wallace, A.L., Ahmed, K., Laxman, S., Campeau, P.M., Lee, B.H., Hutson, S.M., Tu, B.P., Williams, N.S., Tambar, U.K., Wynn, R.M., Chuang, D.T., 2013. Structure-based design and mechanisms of allosteric inhibitors for mitochondrial branched-chain alpha-ketoacid dehydrogenase kinase. Proc. Natl. Acad. Sci. U. S. A. 110, 9728–9733.
van der Velden, D.L., Opdam, F.L., Voest, E.E., 2016. TAS-102 for treatment of advanced colorectal cancers that are no longer responding to other therapies. Clin. Cancer Res. 22, 2835–2839.
Watanabe, A., Higashi, T., Sakata, T., Nagashima, H., 1984. Serum amino acid levels in patients with hepatocellular carcinoma. Cancer 54, 1875–1882.
Wubetu, G.Y., Utsunomiya, T., Ishikawa, D., Ikemoto, T., Yamada, S., Morine, Y., Iwahashi, S., Saito, Y., Arakawa, Y., Imura, S., Arimochi, H., Shimada, M., 2014. Branched chain amino acid suppressed insulin-initiated proliferation of human cancer cells through induction of autophagy. Anticancer Res. 34, 4789–4796.
Yoshikawa, R., Yanagi, H., Shen, C.S., Fujiwara, Y., Noda, M., Yagyu, T., Gega, M., Oshima, T., Yamamura, T., Okamura, H., Nakano, Y., Morinaga, T., Hashimoto-Tamaoki, T., 2006. ECA39 is a novel distant metastasis-related biomarker in colorectal cancer. World J. Gastroenterol. 12, 5884–5889.
Zhang, Y., Zhang, Y., Geng, L., Yi, H., Huo, W., Talmon, G., Kim, Y.C., Wang, S.M., Wang, J., 2016. Transforming growth factor β mediates drug resistance by regulating the expression of pyruvate dehydrogenase kinase 4 in colorectal cancer. J. Biol. Chem. 291, 17405–17416.
Zhu, F., Zykova, T.A., Kang, B.S., Wang, Z., Ebeling, M.C., Abe, Y., Ma, W.Y., Bode, A.M., Dong, Z., 2007. Bidirectional signals transduced by TOPK-ERK interaction increase tumorigenesis of HCT116 colorectal cancer cells. Gastroenterology 133, 219–231.
Zhu, M.M., Xu, X.T., Nie, F., Tong, J.L., Xiao, S.D., Ran, Z.H., 2010. Comparison of immunochemical and guaiac-based fecal occult blood test in screening and surveillance for advanced colorectal neoplasms: a meta-analysis. J. Dig. Dis. 11, 148–160.